The radical ions from bis(2,4,6-tri-*tert*-butylphenyl)-1,3-diphosphaallene. A multi-disciplinary approach and a reassessment

Angelo Alberti,*[a] Massimo Benaglia,[a] Mila D'Angelantonio,[b] Salvatore S. Emmi,[b] Maurizio Guerra,*[a] Andrew Hudson,[c] Dante Macciantelli,[a] Francesco Paolucci[d] and Sergio Roffia[d]

[a] *I.Co.C.E.A. - CNR, Area della Ricerca, Via P. Gobetti 101, I-40129 Bologna, Italy*
[b] *FRAE - CNR, Area della Ricerca, Via P. Gobetti 101, I-40129 Bologna, Italy*
[c] *School of Chemistry, Physics, and Environmental Science, University of Sussex, Brighton, UK BN1 9QJ*
[d] *Dipartimento di Chimica "G. Ciamician", Università di Bologna, Via G. Selmi 2, I-40125 Bologna, Italy*

Received (in Cambridge) 27th July 1998, Accepted 8th December 1998

The radical ions from bis(2,4,6-tri-*tert*-butylphenyl)-1,3-diphosphaallene were investigated through EPR spectroscopy, cyclic voltammetry, and pulse radiolysis. Cyclic voltammetry indicated an oxidation potential of 2.0 V *vs.* SCE and a reduction potential in the range −1.97 to −2.10 V *vs.* SCE, depending on solvent. Whilst the starting compound does not significantly absorb beyond 300 nm, the absorption spectrum of the radical cation is characterised by bands centred at *ca.* 320 and *ca.* 410 nm: according to EOM-CCSD calculations on the unsubstituted diphosphaallene the latter band should be due to a transition from the SOMO to the second LUMO, while the former might result from the overlapping of three different transitions. The EPR spectra recorded in the present study upon reduction of the title compound are far more complex than those recently published, and significant differences have been observed upon chemical or electrochemical reduction. A higher spin density on the phosphorus atoms is observed in the anion than in the cation, in agreement with the different nature of the SOMO in the two species predicted by UB3LYP calculations on the model compound diphenyl-1,3-diphosphaallene, which also predict for both ions the existence of *cis* and *trans* geometrical isomers, the latter being more stable. In both radical ions the unpaired electron is mainly localised in the PCP moiety, namely in a π-allylic type MO in the cation and in a σ MO in the anion. These pictures of the SOMO are opposite to those recently published following MP2 calculations on the unsubstituted diphosphaallene.

Introduction

1,3-Diphosphaallenes are peculiar compounds because of the presence of the two orthogonal carbon–phosphorus double bonds. These compounds are also characterised by a remarkably low stability, and since its first synthesis in the early eighties, bis(2,4,6-tri-*tert*-butylphenyl)-1,3-diphosphaallene[1] **1** remains the only isolated member of the family. This is most probably attributable to protection of the two C=P double bonds by the very bulky trisubstituted aryl rings. The structure of this compound has been investigated through X-ray diffractometric studies:[2] it was found that the P=C=P system slightly deviates from linearity and that the two aryl groups are orthogonal with respect to each other.

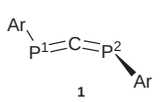

1

Ar = 2,4,6-tri-(*tert*-butyl)phenyl

Ab initio MC-SCF calculations on these compounds were carried out using HP=C=PH as a model,[3] the structure of the only compound actually isolated being forbiddingly complex for this type of approach. Despite the drastic simplifications of the model, the calculations led to results in substantial agreement with the structural investigation.

In the course of our studies on the reactions of organic and organometallic free radicals with unsaturated species, some of us have recently examined the addition of different radicals to diphosphaallene **1** and have established that the regioselectivity of these reactions is strongly dependent on the nature of the attacking radical.[4] Thus it was found that electrophilic alkoxyl (•OR) and alkylthiyl (•SR) radicals attack one of the two equivalent phosphorus atoms affording very short-lived phosphavinyl σ radical adducts with general structure **2**, while radicals centred at a Group IV element such as silicon (•SiR_3), germanium (•GeR_3) or tin (•SnR_3) attack the central carbon atom to give relatively persistent phosphinyl radical adducts with general structure **3** (see Scheme 1).

Scheme 1

We then set out to investigate through a multi-disciplinary approach involving cyclic voltammetry, EPR spectroscopy, pulse radiolysis and MO calculations the radical ions resulting from the one-electron oxidation and one-electron reduction of **1**. We were still in the course of these investigations when a paper[5] appeared reporting an EPR and theoretical investigation of the radical cation from **1** or (**1***),† shortly followed by a second one by the same authors reporting on the corresponding radical anions.[6] We were somewhat surprised to find some

† Starred numbers refer to the diphosphaallene with 100% ^{13}C at the central position.

significant differences from our results at both the experimental (EPR) and theoretical (MO calculations) levels, the disagreement being particularly severe in the case of the reduction. While the conflicting results of the MO calculations might reflect the choice of different models (compound **1** is a very complex system and it must be approximated at least to the diphosphaallene bearing two unsubstituted phenyl rings in order to carry out the calculations), the difference in the EPR spectra can only originate from the use of more favourable experimental conditions. In particular our spectra were characterised by a better resolution and a more complex pattern, the intriguing implications of which could not be overlooked. Besides, although in both previous investigations[5,6] the radical ions were generated through electrochemical procedures inside the cavity of the EPR spectrometer, no clear details were given as to the actual electrochemical behaviour of diphosphaallene **1**. We therefore completed our studies and report here the results of the EPR investigation on the oxidation and reduction of diphosphaallenes **1** and **1***, along with those of the cyclic voltammetry study; the absorption spectrum of the radical cation, generated through pulse radiolysis in CH_2Cl_2 and CCl_4 solutions, is also described. We believe that the present experimental results combined with those of MO calculations provide a clearer cut and, we trust, more correct picture of the radical ions from this interesting diphosphaallene.

Results

Cyclic voltammetry

The electrochemical behaviour of **1** has been studied by cyclic voltammetry at various temperatures in THF, ACN and CH_2Cl_2 containing 0.05 M $(C_2H_5)_4NPF_6$ as supporting electrolyte, using a disc ultramicroelectrode (UME) of 10 μm diameter as working electrode.

Oxidation. The interpretation of the cyclic voltammetric curve (cvc) observed for the oxidation of **1** in THF is rather difficult. However, the higher intensity of the cvc observed in the presence of the diphosphaallene with respect to that for the base solution, just before the discharge of the latter, would indicate the oxidation of **1** to take place at *ca.* 2 V *vs.* SCE.

Fig. 1 (trace a) shows the cvc recorded in CH_2Cl_2 at 25 °C for a scan rate $v = 500$ V s^{-1} utilising the same UME. Due to the low solubility of **1** in this medium and to the oxidation of the base solution, the peaks appearing in the cvc are scarcely evident. However, by subtracting the current due to the base solution, the curve (b) is obtained which clearly exhibits an oxidation peak Ia together with a cathodic peak Ic. The couple of peaks Ia/Ic can be confidently attributed to the redox couple **1/4**, on the basis of the results of the digital simulation of the cvc and of the comparison with the behaviour of a suitable internal standard. As a matter of fact, the digital simulation of the curve shows that the higher value found for the difference between the cathodic peak potential $E_{p,c}$ and the anodic peak potential $E_{p,a}$ for the couple of peaks Ia/Ic with respect to that expected for the one-electron reversible process $\mathbf{1} = \mathbf{4} + e^-$, is compatible with the uncompensated ohmic potential drop of the relevant medium. The number of electrons involved in the process, *i.e.* one, was obtained as described in the Experimental section. The lower intensity of the cathodic peak Ic as compared to that of the anodic peak Ia, along with the presence of inflections in the reduction pattern at potentials more negative than that corresponding to peak Ic, suggest that the radical cation **4** is very short lived, either owing to its fragmentation or to its participation in a chemical reaction. A digital simulation of the cv curve (b) in Fig. 1 was carried out hypothesising that oxidation is followed by an irreversible first-order reaction (EC mechanism) and assuming that the product of such a reaction is also electroactive (at more negative potentials). The simulated

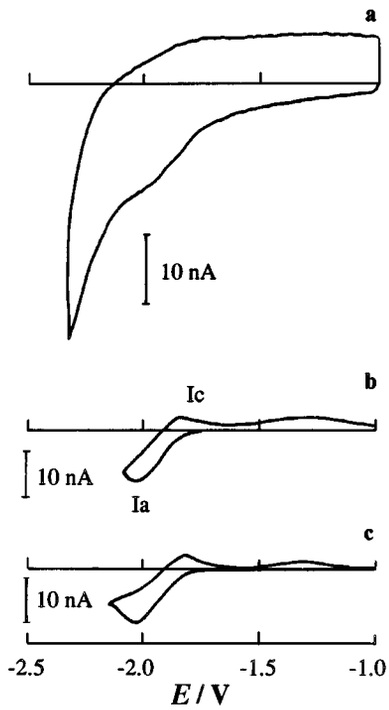

Fig. 1 (a) Cyclic voltammetric curve observed at 25 °C for **1** in methylene chloride at a scan rate $v = 500$ V s^{-1}; working electrode: Pt UME with a 10 μm diameter. (b) Curve obtained by subtracting from curve (a) the current due to the base solution. (c) Digital simulation of curve (b).

curve (c) agrees quite satisfactorily with the experimental trace, providing support to the proposed electrode mechanism. A value of $E_{1/2}(\mathbf{1/4}) = 1.93$ V was obtained, while the rate constant for the decay of the cation was estimated as $k_{EC} = 10^3$ s^{-1}.

Reduction. Fig. 2 shows the cvc's recorded in THF at −70 °C (a) and 25 °C (d) with a scan rate $v = 100$ V s^{-1}, while curves (b) and (e) result from subtraction of the contributions due to the base solution. Under the experimental conditions this scan rate is close to the upper limit beyond which severe distortions of the curves occur due to capacitive current and to an uncompensated ohmic potential drop in solution. Curves (b) and (e) exhibit two cathodic peaks Ic and IIc, with relative heights dependent on temperatures. At −70 °C, anodic partners Ia and IIa are observed for both cathodic peaks, their lower height with respect to that of the latter peaks providing an indication of the occurrence of irreversible chemical reactions coupled to the electron transfer. Through the same procedure used in the oxidation, both the electrochemical steps were found to correspond to one-electron processes, and on this basis the two reduction peaks have been associated with the formation of the diphosphaallene radical anion **6** and diamagnetic dianion **7**, respectively. Besides peaks Ia and IIa, small additional peaks, whose pattern depends on whether the scan is inverted after the first or the second reduction peak, and appearing as inflections in the voltammetric curve are observed in the oxidation scan. The lower intensity of peaks Ia and IIa as compared to that of peaks Ic and IIc and the presence of the additional anodic peaks are a clear indication that chemical reactions are coupled to both the reduction processes. Information about the reactions taking place have been obtained from the dependence of the cvc's on temperature and scan rate. In particular, as the temperature is increased, peak IIc decreases, becoming very small at 25 °C, at which temperature peak Ic always appears chemically irreversible for the experimentally adopted scan rate. The height of IIc also decreased on decreasing the scan rate at a given temperature.

The overall reduction process outlined in Scheme 2 is proposed in order to explain the observed behaviour. Curves (c)

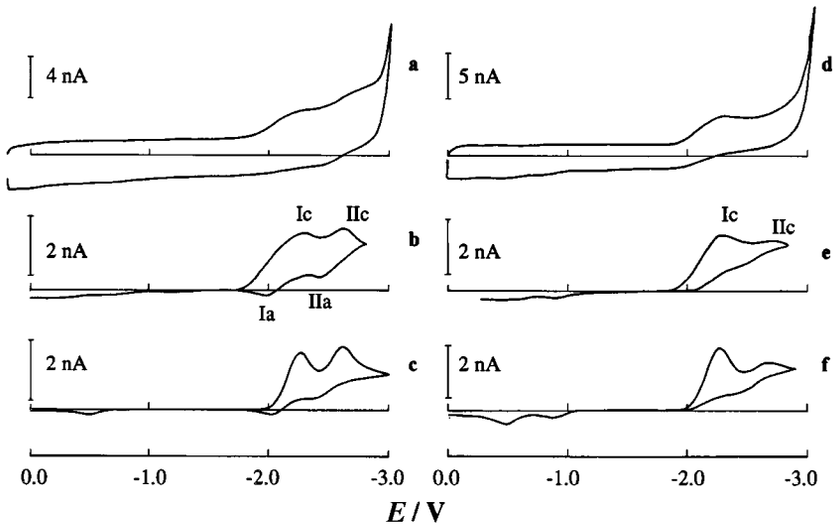

Fig. 2 (a) Cyclic voltammetric curve observed at −70 °C for **1** in THF at a scan rate $v = 100$ V s^{-1}; working electrode: Pt UME with a 10 μm diameter. (b) Curve obtained by subtracting from curve (a) the current due to the base solution. (c) Digital simulation of curve (b). (d) The same as for curve (a), but at $T = 25$ °C. (e) Curve obtained by subtracting from curve (d) the current due to the base solution. (f) Digital simulation of curve (e).

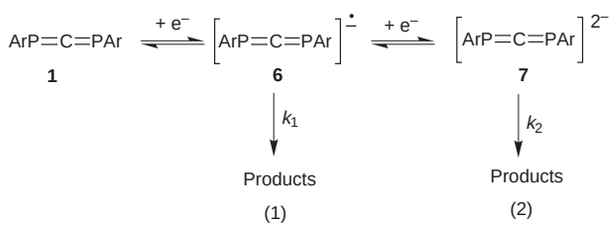

Scheme 2

and (f) shown in Fig. 2 were calculated assuming that the reduction process proceeds as outlined in Scheme 2. These simulated curves were in substantial agreement with the experimental traces (b) and (e), respectively, and led to values of $E_{1/2}$(**1**/**6**) = −2.05 V, $E_{1/2}$(**6**/**7**) = −2.45 V, $k_1 = 300$ s^{-1}, and $k_2 = 800$ s^{-1}. From the slope of the linear Arrhenius plot obtained through the simulation of cvc's at different temperatures, the same activation energy value was derived for the two processes, *i.e.* $E_a = 8 \pm 2$ kcal mol^{-1}.

The CV behaviour of **1** in ACN, a solvent where the faradaic-to-capacitive current ratio is more favourable owing to the greater solubility of the compound and where the lower resistivity allows the use of higher scan rates thus permitting a better characterisation of the electrode process, provided further support for the proposed mechanism for the reduction of **1**. At 25 °C with $v = 1000$ V s^{-1} two one-electron reduction peaks were evidentiated upon subtraction of the contribution of the base solution, the first being reversible and the second irreversible at the accessible scan rates (see Fig. 3). The analysis of the CV behaviour as a function of scan rate, temperature and reversal potential was again found consistent with the mechanism shown in Scheme 2, and the simulated curves calculated accordingly led to values of $E_{1/2}$(**1**/**6**) = −2.02 V, $E_{1/2}$(**6**/**7**) = −2.25 V, $k_1 = 1000$ s^{-1}, and $k_2 = 5000$ s^{-1}.

EPR Spectroscopy

Both the radical cation and the radical anion of the diphosphaallene **1** (or **1***) could be directly observed by means of EPR spectroscopy. Although temperature did not seem to significantly affect the persistence of the cation signal, in our experiments it proved critical in the case of the alkali metal reduction.

The best spectra of radical cations **4** (or **4***) were obtained by chemical oxidation, *i.e.* by adding a small amount of iodosobenzene bis(trifluoroacetate), IBTFA, to a thoroughly argon purged solution of **1** (or **1***) in 1,1,1,3,3,3-hexafluoropropan-2-ol[7] (HFP) at room temperature. In this case the signal (see Fig. 4a) consisted of a 1:2:1 triplet (3.21 mT) due to the two phosphorus nuclei, each line being further split into a multiplet with an apparent line separation of 0.118 mT because of the interaction of the unpaired electron with protons of the two 2,4,6-tri-*tert*-butylphenyl moieties (see Table 1). When starting from **1*** a doublet splitting (3.71 mT) from the ^{13}C nucleus was also observed. Several computer simulated spectra produced with different sets of parameters satisfactorily matched the experimental pattern: it was thus impossible to establish whether the observed hyperfine structure is originated by coupling of the unpaired electron with all the hydrogens from the *tert*-butyl groups as well as the *meta* aromatic hydrogens, or only by coupling with the hydrogens of the *ortho tert*-butyl groups.

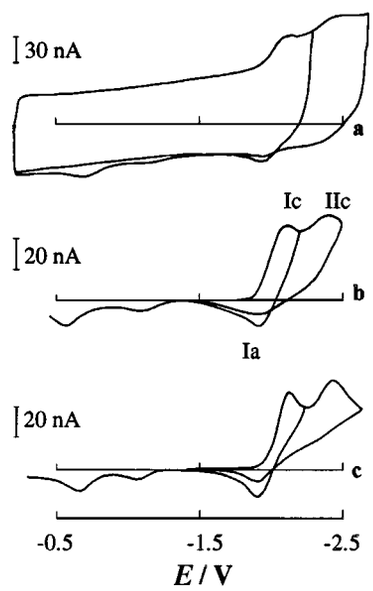

Fig. 3 (a) Cyclic voltammetric curve observed at 25 °C for **1** in ACN at a scan rate $v = 1000$ V s^{-1}; working electrode: Pt UME with a 10 μm diameter. (b) Curve obtained by subtracting from curve (a) the current due to the base solution. (c) Digital simulation of curve (b).

Electrochemical oxidation (*ca.* 2.0 V *vs.* SCE) of **1** (or **1***) in THF inside the cavity of the EPR spectrometer led to the observation of spectra (a 1:2:1 triplet) of the radical cation **4** (a 1:~3:~3:1 quartet for **4***) that were substantially consistent with those already reported (see Table 1), although indicative of

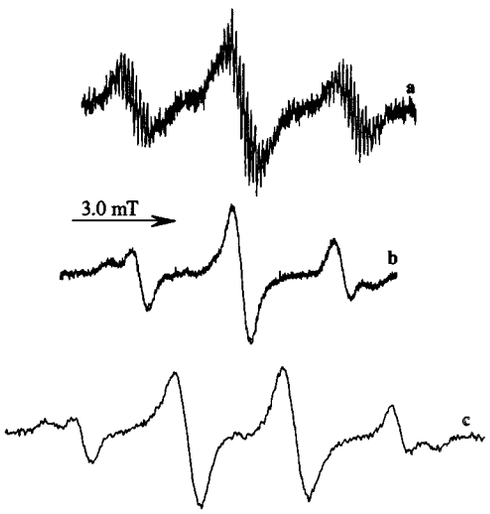

Fig. 4 EPR spectra observed upon oxidation of **1** with IBTFA in HFP (a), and electrochemical oxidation of **1** (b) and **1*** (c) in methylene chloride.

a further hyperfine structure that could not be properly resolved.[5] On the other hand, when THF was replaced with methylene chloride the observed spectra indicated the simultaneous presence of two radicals (see Figs. 4b and 4c) with spectra characterised by rather different linewidths but exhibiting nearly identical *g*-factors and similar couplings with the two phosphorus atoms and the carbon-13 nucleus. The two species were present in comparable amounts and did not exhibit any significant variation of the spectral pattern when the temperature was varied.

The electrochemical reduction of 10^{-3} M THF solutions of **1** (and **1***) resulted in the detection of spectra consistent with those observed previously (see Fig. 5a), *i.e.* an unusually shaped 1 : 2 : 1 triplet (triplet of doublets), exhibiting two outer lines much broader than the central one(s), only under low resolution conditions (high magnetic field modulation, *i.e.* 0.25 mT). At variance with the previous report,[6] the narrower central line (or doublet) clearly exhibited signs of an additional doublet splitting, which became more evident by lowering the field modulation to 0.075 mT (see Fig. 5b). A further reduction of the field modulation (0.0075 mT) revealed the existence of a far more complex hyperfine pattern (Fig. 5c), indicating interaction of the unpaired electron with some of the hydrogens of the 2,4,6-tri-*tert*-butylphenyl moieties. The dependence of the spectral pattern on temperature paralleled that already described, and below −30 °C the outer lines of the triplet were broadened beyond detection. The spectra may be viewed either as the overlapping of two independent signals, *i.e.* a broad triplet (triplet of doublets) and a sharper singlet (doublet) with a slightly lower *g*-factor, or as a 1 : 2 : 1 triplet (triplet of doublets) due to a single radical with broad outer lines and with the central line (doublet) that, owing to a second order splitting of *ca.* 0.18 mT, is partially resolved into its nuclear singlet and nuclear triplet components, the former being much narrower than the latter.

We wish to emphasise that in all our experiments disconnecting the electrolytic apparatus (two electrode cells of different geometry, see Experimental) from the power source resulted in a remarkable increase of the intensity of the EPR signals which remained detectable for up to several hours.

Rather surprisingly, absolutely identical EPR spectra were obtained by similar electrochemical reduction of 3,3-dichloro-1,2-diphosphiranes **8** (or **8***), intermediates in the synthesis of **1** (or **1***).

When the electrolytic experiments were carried out by using voltages between −2.5 and −5.0 V, a very strong, long-lived and well resolved 1 : 2 : 1 triplet was observed, which proved

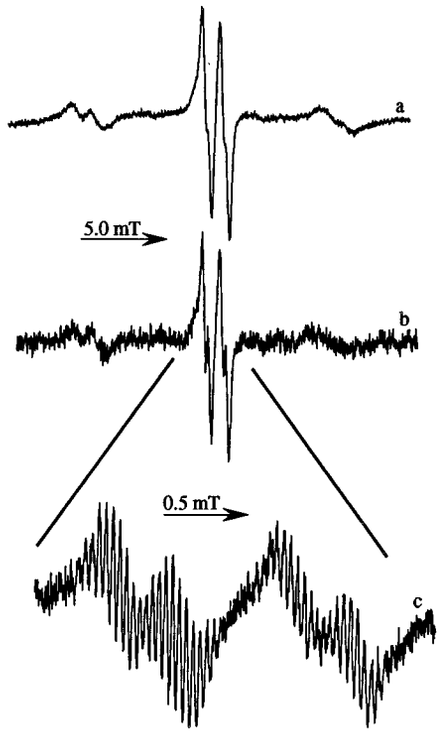

Fig. 5 EPR spectra observed upon electrolytic reduction at room temperature of 10^{-3} M THF solutions of **1*** with different field modulation amplitude (ma) settings: (a) ma = 0.25 mT; (b) ma = 0.1 mT; (c) expanded central group recorded with ma = 0.075 mT.

independent of the nature of the starting compound. This signal originated from a radical where the unpaired electron is coupled with two nuclei having spin $I = 1/2$ ($a = 0.176$ mT), with a set of 18 equivalent hydrogens ($a_{18H} = 0.007$ mT), a set of nine equivalent hydrogens ($a_{9H} = 0.036$ mT) and characterised by a *g*-factor of 2.0049_3. Under high field modulation conditions, the triplet signal collapsed to an intense single line. The very small value of the triplet splitting and the absence of any effect from the ^{13}C nucleus when using **1*** could hardly be reconciled with the starting diphosphaallene, and we attribute this signal to an adventitious species **9** that, despite the reducing nature of the medium, we identify as the 2,4,6-tri-*tert*-butylphenoxyl radical, whose known spectral parameters account very satisfactorily for the observed spectrum.[8]

A single narrow line with a *g*-value close to that of the free electron was observed upon reaction of **1** (or **1***) with a lithium–mercury amalgam in THF at $T \leq -40$ °C, either in the absence or in the presence of some 12-crown-4 ether; the same spectra observed upon electrochemical reduction in THF and due to radical **6?** (or **6?***) were instead observed at $T \geq -40$ °C. In open contrast with this finding and with the previous report,[6] very different EPR spectra were observed by allowing **1** (or **1***) to react with a sodium–potassium alloy mirror in THF at very low temperature. In this case the spectrum consisted of a normal 1 : 2 : 1 triplet, further split into smaller doublets in the case of the ^{13}C-enriched substrate (see Table 1 and Fig. 6a,b), and is believed to reflect the formation of a radical ion pair **10** (or **10***) between the radical anion from the diphosphaallene and an alkali counterion. This spectrum was critically dependent on temperature: in order to observe it, the reaction of the diphosphaallene solution with the metal mirror had to be carried out at or below 193 K. The presence of some dibenzo-18-crown-6 ether was also necessary in order to complex the alkali counterion formed in the reduction.[9] Once the ion pair had been generated, its spectrum remained visible on raising the temperature but its intensity became vanishingly small above 243 K. If the sample was allowed to warm to room temperature, the signal due to the 2,4,6-tri-*tert*-butylphenoxyl radical **9** developed again with time. In no case did re-cooling of the solution result

Table 1 EPR Hyperfine spectral parameters (hfs constants in mT) for the radical ions observed upon chemical or electrochemical oxidation and reduction of **1***

Method	Solvent	Radical	Amount (%)	$a_{^{31}P}$	$a_{^{13}C}$	g	T/K
Chem. Ox.[a,b]	HFP–IBFA	**4***	100	3.21	3.71	2.0026_6	298
El. Ox.[5]	THF	**4***	100	3.10	3.10	2.0025_0	298
El. Ox.[a]	THF	**4***	100	3.05	3.20	2.0026_4	298
El. Ox.[a]	CH_2Cl_2	**4***[c]	53.5	3.02	3.35	2.0026_5	298
El. Ox.[a]	CH_2Cl_2	**5***[c]	46.5	3.6	3.50	2.0026_5	298
El. Red.[6]	THF	**6*?**	100	7.64	0.96	2.009	298
El. Red.[a,b]	THF	**6*?**	100	7.68	1.09	2.0086_5	298
Na/K Red.[a]	THF	**10***	100	6.20	1.45	2.0048_3	193

[a] This work. [b] Additional hyperfine structure from an undefined number of hydrogen atoms: see text. [c] The couplings of radicals **4*** and **5*** in methylene chloride can be interchanged.

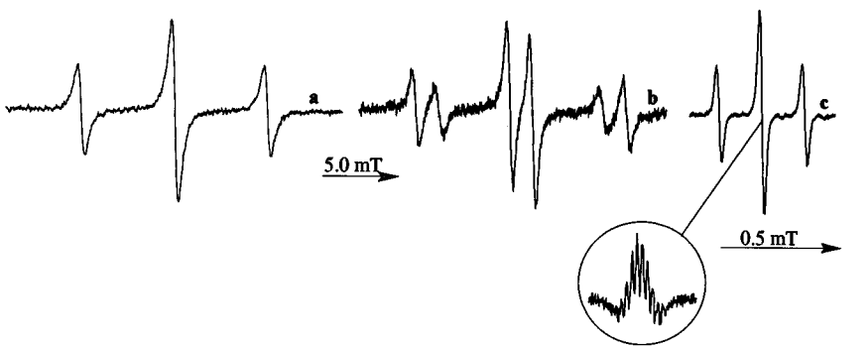

Fig. 6 Spectra observed upon metal reduction of **1** (a) and **1*** (b) in THF at 193 K, and at room temperature (c) with the expanded second derivative of the central line.

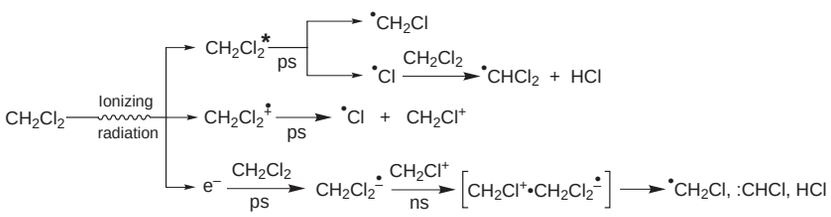

Scheme 3

in the reappearance of the spectrum of **10** (or **10***), thus indicating that one of the partners of the ion pair, namely the radical anion, is irreversibly degraded as the temperature is raised. The observation of **9** suggests that loss of an aromatic moiety is among the possible decay pathways.

Pulse radiolysis

Oxidation of **1** to its radical cation **4** could also be achieved by pulse radiolysis (PR) in electron scavenging solvents like chloromethanes, *i.e.* CCl_4 or CH_2Cl_2, and the combination of UV–vis kinetic absorption spectrometry with pulse radiolysis (PR-KAS) allowed its spectral characterisation and the determination of its stability at room temperature, as well as the monitoring of the formation process of the radical cation and of the reactions in which it could possibly be involved.

Pulse radiolysis is based on the effects of a wave of fast electrons crossing a material. The process, which is outlined in Scheme 3, results in the generation of excitations and ionisations. In particular the interaction of radiation with methylene chloride produces the excited molecule, CH_2Cl_2*, the radical cation, $CH_2Cl_2^{+\bullet}$, and the corresponding electron, e^-. The electrons escaping the electric field of the positive ions are captured by other methylene chloride molecules in an electron attachment process which eventually results in the production of chloride ions and neutral radicals. It must be emphasised that, at variance with what is found in water or other polar solvents, no solvated electrons capable of directly acting as reducing agents are isolated in chlorinated solvents. The radical cation $CH_2Cl_2^{+\bullet}$ after a few picoseconds fragments to the closed shell CH_2Cl^+ cation and a chlorine atom, which can abstract hydrogen producing HCl and dichloromethyl radicals. While for the purpose of our investigation HCl can be ignored, particular attention has to be paid in order to avoid the chlorination of **1** by chlorine atoms, which are very reactive towards π systems. Experimentally this is achieved by keeping the solute concentration below 10^{-3} M; under these conditions chlorine atoms are consumed through hydrogen abstraction from the solvent in less than 100 ns ($k \approx 1.04 \times 10^7$ dm^3 mol^{-1} s^{-1}).[10,11]

The species involved in electron transfer reactions are the cationic fragment CH_2Cl^+ and the chloro-substituted radical, $CHCl_2^{\bullet}$ (CCl_3^+ and $CCl_3^{\bullet}$, respectively, for CCl_4). Due to its very high electron affinity, CH_2Cl^+ acts as a strong oxidising agent towards the majority of organic materials; if the oxidation potential of the solute is low, dichloromethyl $CHCl_2^{\bullet}$ and trichloromethyl $CCl_3^{\bullet}$ radicals can also be responsible for oxidation processes. Although it is known that electron transfer between the ionic fragments CH_2Cl^+ or CCl_3^+ and aromatic π systems can occur at ultra-diffusional rates,[12] we have observed that this type of electron transfer is not efficient in the presence of **1**, the ionic fragments following instead their natural annihilation with the molecular anion (see Scheme 3). Indeed, as is explained in detail in the following sections, oxidation of **1** occurs on a longer time scale.

Oxidation in CH_2Cl_2. The UV–vis absorption spectrum of **1** in CH_2Cl_2 exhibits two strong absorption maxima at 225 and 275 nm and a weak one at 350 nm [see Fig. 7(a)]. After irradiation with electron pulses it showed a dramatic change with

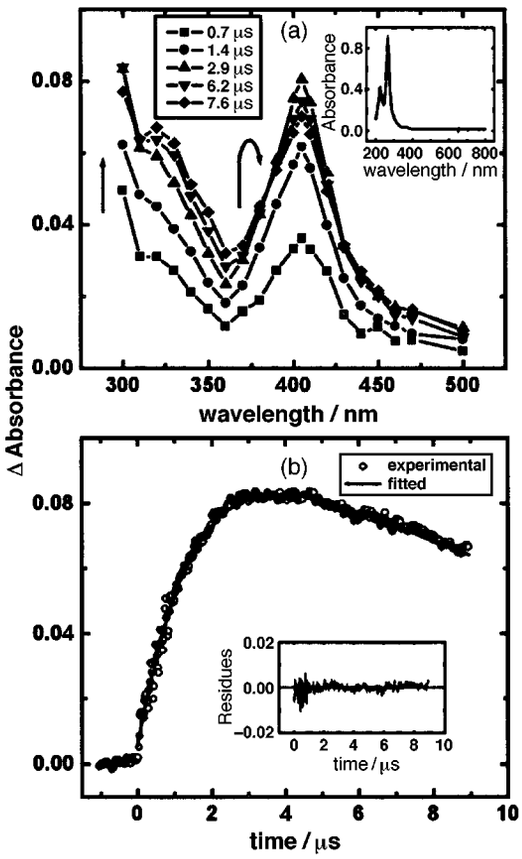

Fig. 7 (a) Time resolved absorption spectra observed during pulse radiolysis of **1** in argon purged CH_2Cl_2. Inside the frame: time elapsed after the pulse. An isosbestic point is present at 385 nm. [**1**] = 0.98×10^{-4} M, optical path = 2 cm, normalised dose = 109 Gy. Inset: original absorption spectrum of [**1**] = 1.60×10^{-4} M in CH_2Cl_2, optical path = 0.1 cm. (b) Pulse radiolysis oxidation in CH_2Cl_2. Scatter line: optical curve obtained at 405 nm by irradiating a sample of [**1**] = 9.8×10^{-5} M saturated with argon, optical path = 2 cm, pulse duration = 50 ns, irradiation dose = 109 Gy. Full line: best non-linear fitting of a two-consecutive-first-order reaction model, fast component, $k = 6.23 \times 10^5$ s^{-1}, slow component, $k = 7.21 \times 10^4$ s^{-1}. Inset: residual errors between experimental and fitted values.

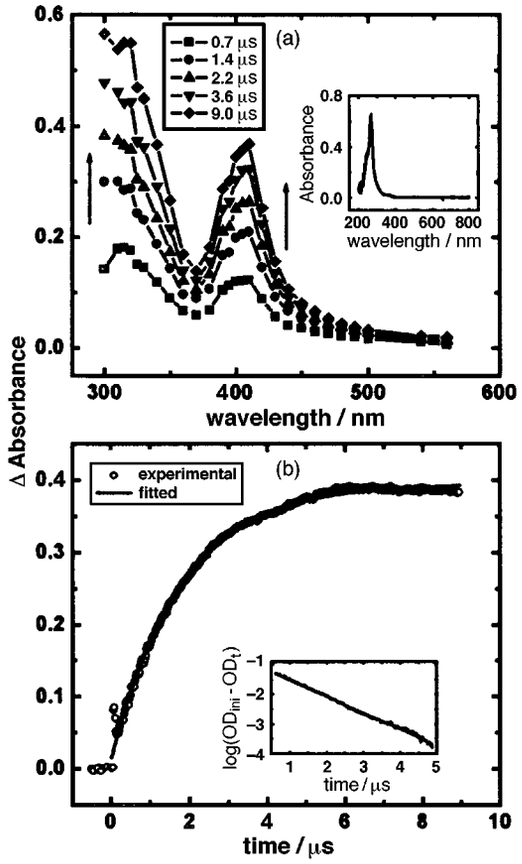

Fig. 8 (a) Time resolved spectra during pulse radiolysis of **1** in argon purged CCl_4. Inside the frame: time elapsed after the pulse. No isosbestic points can be seen. [**1**] = 1.01×10^{-4} M, optical path = 2 cm, normalised dose = 112 Gy. Inset: original absorption spectrum of [**1**] = 1.52×10^{-4} M in CCl_4, optical path = 0.1 cm. (b) Pulse radiolysis oxidation in CCl_4. Scatter line: optical curve obtained at 405 nm by irradiating a sample of [**1**] = 1.01×10^{-4} M saturated with argon. Optical path = 2 cm, pulse duration = 50 ns, irradiation dose = 122 Gy. Full line: curve obtained by fitting linearly a first-order reaction model. Inset: linear fitting, slope = 5.70×10^5 s^{-1}.

new absorptions centred at 320 and 405 nm. The time evolution of the spectrum demonstrated the lack of persistence of the latter band and the continuous growth of the one centred at 320 nm, while in the period between 3 and 8 μs an isosbestic point emerged at 385 nm. Fig. 7(b), showing the variation of absorbance at 405 nm observed during the oxidation of **1**, suggests that the reaction does not reach completion, because the first formed species immediately transforms into the less absorbing cation **4**. An analysis of the trace using a non-linear fit routine reveals that the overall process can be divided into two stages, with rate constants of 6.36×10^9 dm^3 mol^{-1} s^{-1} and 7.21×10^4 s^{-1}, respectively.

Oxidation in CCl_4. The formation of the cation **4** in CCl_4 is a cleaner process than in CH_2Cl_2. As shown in Fig. 8(a), there is a continuous increase in the optical density from 300 to 550 nm, with two bands peaking at 315 and 410 nm. Fig. 8(b) shows the time evolution of the absorbance at 410 nm together with the linear fitting analysis. The rapidly decaying spike at the beginning of the oxidation curve is attributed to the fast natural annihilation of CCl_3^+ which absorbs in this region. A bimolecular rate constant $k_3 = 5.64 \times 10^9$ dm^3 mol^{-1} s^{-1} for the formation of **4** could be derived from the slope of the linear fitting.

The finding that the optical density in CCl_4 is about 4 times higher than in CH_2Cl_2, is a consequence of the different radiation yields of the oxidising radicals in the two solvents.

MO Calculations

Molecular orbital (MO) calculations have been performed to get information on the structure and the ^{13}C and ^{31}P hyperfine splitting constants of the 1,3-diphosphaallene radical ions and on the nature of the optical transitions observed in the UV–vis region of the radical cation.

In our recent studies on the structural and magnetic properties of localised organic and organometallic radicals we have found[13] that experimental hfs constants can be closely reproduced by *ab initio* methods with moderate-sized basis sets estimating electron correlation effects simply with the Møller–Plesset perturbation theory at second order (MP2) when the doublet state is described by one dominant electronic configuration. Otherwise, the quadratic configuration interaction method with single and double substitutions (QCISD), which requires much more computational resources, must be used to obtain reliable hfs constants.[14] Unfortunately, calculations at the UMP2 level on systems as large as the title diphosphaallene are prohibitive, even if the trisubstituted aryl groups are replaced by simple phenyls in order to simulate the electronic properties of the aryl groups and to partially account for their steric hindrance. It was recently shown[15] that through the use of the density functional theory (DFT) at the UB3LYP level reliable EPR hfs constants can be computed with a modest computational effort, although the average deviation from experiment is slightly larger than that obtained with the UQCISD method.[16] We have therefore carried out calculations

Table 2 Optimum structural parameters[a] and relative stabilities for the *cis*-like and *trans*-like conformations of the HPCPH radical cation computed with different methods employing the 6-311(d,p) basis set

Method	r(P–C)	r(P–H)	∠CPC	∠HPC	ω(HPPH)	ΔE/kcal mol^{-1}
cis-like						
UB3LYP	1.658	1.433	164.4	94.2	45.3	0.0
UQCISD	1.666	1.421	163.8	93.7	45.0	0.0
MCSCF[b]	1.668	1.433	157.3	95.6	47.0	0.0
trans-like						
UB3LYP	1.655	1.433	179.7	94.5	133.4	0.61
UQCISD	1.665	1.421	179.7	93.9	133.6	0.63
MCSCF[b]	1.665	1.433	178.9	95.7	132.9	0.50

[a] Bond lengths in angstroms, bond and dihedral angles in degrees. [b] From ref. 5.

on the diphenyl-1,3-diphosphaallene Ph–P=C=P–Ph and on its radical ions at this level of theory.

Structures. The structural parameters P=C = 1.645 Å (1.633), ∠PCP = 174.3° (172.6), ∠CPC$_{Ph}$ = 100.8° (100.1) of the neutral diphenyl derivative (C_2 symmetry) computed at the B3LYP/6-311G(d,p) level of theory are in accord with the corresponding averaged values determined for **1** by X-ray diffraction[2] reported in parentheses. In particular, the cumulenic structure of the PCP moiety constrains the two phenyl rings to be nearly perpendicular with respect to each other [the torsion angle ω(C^{Ph1}P^{1}P^{2}C^{Ph2}) between the C^{Ph1}–P^1 and C^{Ph2}–P^2 bonds is computed to be 89.2°] as observed experimentally. Ionisation removes the molecular orbital constraint so that steric hindrance could be important in determining the structural parameters. Semiempirical calculations performed on **1** at the AM1 level showed[6] that in the anion **6** the planes of the substituted aryl groups are nearly orthogonal to the CPC$_{Ar}$ plane. The same arrangement of the aryl groups has been obtained by us in preliminary calculations performed on the radical cation **4** at this semiempirical level of theory. Thus, in the DFT calculations on the model diphenyl-1,3-diphosphaallene radical ions we have kept the phenyl groups frozen in this conformation to simulate the steric hindrance of the *tert*-butyl groups.

Upon full optimisation of the other structural parameters of the radical cation the phenyl groups initially tend to assume a full *trans* configuration ($\omega \approx 180°$); subsequently, the ring carbon atom linked to P^1 strongly interacts with the central carbon atom to form a three-membered ring [r(C–C^{Ph1}) = 1.535 Å, ∠CP^{1}C^{Ph1} = 46.7°]. At variance with experiment, the hfs constants computed for the cyclic structure predict two largely different $a_{^{31}P}$ splittings ($a_{^{31}P1}$ = 1.14, $a_{^{13}C}$ = −1.18, and $a_{^{31}P2}$ = 3.38 mT). The steric hindrance exerted by the trisubstituted aryl group should hamper this strong asymmetric interaction in the radical cation of bis(2,4,6-tri-*tert*-butylphenyl)-1,3-diphosphaallene.

We then re-optimised the radical cation enforcing a C_2 symmetry and assuming the phenyl rings to have a hexagonal structure. Under this symmetry constraint, the radical cation in its more stable arrangement adopts a full *trans* conformation (ω = 180°), with a linear PCP backbone. A local minimum corresponding to a *cis*-like structure was computed to lie 2.3 kcal mol^{-1} higher in energy, with a barrier of 9.6 kcal mol^{-1} between the two conformers. In this *cis*-like arrangement the PCP fragment is significantly bent (∠PCP = 166.9°) and the two substituents are sizeably rotated with respect to each other (ω = 46.8°). These results disagree with those previously obtained through MCSCF/6-311G(d,p) calculations carried out on the unsubstituted HPCPH radical cation (C_2 symmetry),[5] which predicted the *trans* structure to have the two substituents rotated with respect to each other by only 132.9° and to be less stable than the *cis*-like structure (ω = 47°). Because of this discrepancy, we then carried out UB3LYP and UQCISD calculations on the HPCPH radical cation to compare the theoretical results obtained at different levels of theory. Interestingly, Table 2 shows that the structural and energetic properties of this radical cation computed both at the UB3LYP and UQCISD levels are in accord with those determined previously employing the MCSCF method. The energy barrier for the *cis*→*trans* isomerisation (9.51 and 8.73 kcal mol^{-1}, respectively) is similar to that computed previously at the CASSCF/6-31G(d,p) level.[5] This indicates that the approximation of replacing the aryl groups with hydrogens is too drastic because the electronic effect of the phenyl groups largely influences the structural properties of the radical cation.

Optimisation of the radical anion (C_1 symmetry) shows that the addition of an electron produces a rotation of the phenyl groups around the C–P bond similar to that found in the radical cation. The radical anion is predicted to adopt a C_2 *trans*-like conformation (ω = 140.5°), the P–C–P backbone being nearly linear (∠PCP = 177.0°), as found for the radical cation. A local minimum with a *cis*-like structure (C_2 symmetry, ω = 45.0°) lies only 0.03 kcal mol^{-1} higher in energy separated by an energy barrier of 8.1 kcal mol^{-1}. These results are again in contrast with those obtained previously on the unsubstituted HPCPH radical anion[6] which predicted the C_2 symmetric structure to be a transition state between two equivalent and rapidly interconverting C_1 asymmetric structures. It should be remarked that in the unsubstituted HPCPH radical anion the stability of the two isomers is reversed as is found for the radical cation, the *cis*-like conformer being computed to be more stable than the *trans*-like conformer by 0.24 kcal mol^{-1}.

All in all, the present calculations suggest that only the full *trans* conformers should be thermally populated in the bis-(2,4,6-tri-*tert*-butylphenyl)-1,3-diphosphaallene radical cation **4**, whereas in the corresponding radical anion **6** both the *cis*-like and *trans*-like conformers should be detectable.

Electronic configuration. The hyperfine structure of these radical ions depends mainly on the shape of the singly occupied MO (SOMO). The previous spatial representation of the SOMO of the unsubstituted HPCPH radical ions appears to be different from that found in our calculations for both ions from PhPCPPh, and a brief discussion on this point is necessary.

According to our calculations the unpaired electron in the PhPCPPh radical cation occupies a π allylic-type non-bonding MO. There are three electrons in the π allylic framework and four electrons on the σ framework mainly localised at the P atoms.

The electronic configuration of the frontier MOs can be represented as

$$\sigma n_{P+}{}^2, \sigma n_{P-}{}^2, \pi^2, \pi_{nb}{}^1, \sigma_C{}^0, \pi^{*0}$$

where σn_{P+} and σn_{P-} are the in-phase and out-of-phase combinations of the phosphorus lone pairs, σ_C is mainly localised to the $2p\sigma_C$ orbital of the central carbon atom, π, π_{nb} and π* are the π allylic-type MOs. In σ_C the $2p\sigma_C$ orbital is significantly mixed with the phosphorus lone pairs.

Table 3 Optimum structural parameters[a] and relative stabilites for the *trans*-like conformation and the full *trans* conformation in the σ and π electronic configurations of the HPCPH radical anion computed at the UQCISD/6-311G** level

	r(P–C)	*r*(P–H)	∠CPC	∠HPC	ω(HPPH)	Δ*E*/kcal mol^{-1}
trans-like	1.677	1.428	178.0	101.4	147.0	0.0
Full *trans* (σ)	1.683	1.426	180.0	100.6	180.0	0.0
Full *trans* (π)	1.653	1.471	180.0	108.1	180.0	30.6

[a] Bond lengths in angstroms, bond and dihedral angles in degrees.

In the previous calculations, the σ- and π-type MOs in the populated conformers (*cis*-like and *trans*-like) were found to be mixed.[5] However, the spin populations ρ reported for the HPCPH cation (ρ_C *ca.* 0.49 and ρ_P *ca.* 0.18 for both conformers) suggest that the electronic configuration should be represented by

$$\sigma n_{P_+}{}^2, \sigma n_{P_-}{}^2, \pi^2, \sigma_C{}^1, \pi_{nb}{}^0, \pi^{*0}$$

that is, there are five electrons of σ-type and two electrons of π allylic-type.

Our calculations show that in the anion the unpaired electron occupies the σ_C MO. Although the σ and π MOs are partially mixed at the minimum, the electronic configuration can be approximately represented by

$$\sigma n_{P_+}{}^2, \sigma n_{P_-}{}^2, \pi^2, \pi_{nb}{}^2, \sigma_C{}^1, \pi^{*0}$$

Also in this case the spatial representation of the SOMO (σ-like configuration) is in contrast with that described previously in which the unpaired electron occupies a π allylic-type non-bonding MO (π-like configuration) where the negative charge should be located on the central carbon atom:

$$\sigma n_{P_+}{}^2, \sigma n_{P_-}{}^2, \pi^2, \sigma_C{}^2, \pi_{nb}{}^1, \pi^{*0}$$

We have already shown that the radical cation has a pure π configuration, where the σ and π orbitals are not mixed, since the energy minimum occurs in the full *trans* conformation. A similar electronic configuration might be obtained in the anion adding two electrons to the low-lying σ_C MO (empty in the cation). This electronic arrangement is, however, expected to be much less stable than the one in which one electron is added to the σ_C empty MO and the other one to the SOMO (π_{nb}).

The optimised structural parameters for the unsubstituted HPCPH radical anion have been compared with those obtained for the two electronic σ and π configurations in the full *trans* conformation, where they are not mixed, to firmly establish the nature of the electronic configuration in the radical anion. Table 3 shows that at the UQCISD/6-311G** level the optimum structural parameters at the *trans*-like minimum are similar to those optimised for the σ electronic configuration but largely different from those optimised for the π electronic configuration.

It should be noted that the σ configuration in the full *trans* conformation is computed to be more stable than the π configuration by 29.8 kcal mol^{-1} and lies only 0.8 kcal mol^{-1} higher in energy than the *trans*-like minimum. These findings are in line with the simple MO considerations reported above and indicate that the diphosphaallene radical anion has a σ-like electronic configuration.

^{13}C and ^{31}P hfs constants. The values of theoretical hyperfine coupling constants should be averaged over the thermally populated vibrational states. Significant vibrational contributions to the hfs constants derive from rotation or inversion motions having energy barriers less than 3 kcal mol^{-1}.[17] Thus, the effect of the Boltzmann average over the rotational states for the *trans*→*cis* isomerisation on the value of the hfs constants should be small since the energy barrier to rotation is computed to be sizeable in both ions (>8 kcal mol^{-1}). In the *trans*-like conformer of the radical anion the energy barrier to the roto-inversion motion connecting two equivalent conformations is however computed to be only 2.9 kcal mol^{-1}. Thus, the hfs values has been averaged over this mode.

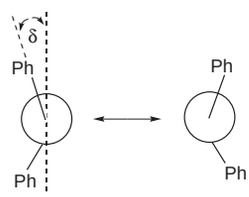

(Roto-inversion motion)

In the cation the ^{31}P hfs constant ($a_{^{31}P}$ = 3.24 mT) computed at the absolute minima, *i.e.* for the full *trans* structure, is in good accord with that experimentally observed, whereas calculations largely underestimate the ^{13}C constant ($a_{^{13}C}$ = −1.45 mT). The significant discrepancy with experiment should be ascribed to a deficiency of the model radical in balancing electronic and steric effects present in the trisubstituted aryl groups (see above). These theoretical hfs values are significantly different from those computed previously from projected UMP2 spin density (PMP2/6-311G**) for the unsubstituted HPCPH radical cation in the *trans*-like conformation ($a_{^{13}C}$ = 3.0 mT, $a_{^{31}P}$ = 5.03 mT). In the light of the present calculations the arithmetical average over ω in the range 10–170° ($a_{^{13}C}$ = 4.3 mT, $a_{^{31}P}$ = 3.50 mT) reported in the same study does not have any physical meaning corresponding to a free rotation motion about the C–P bonds. The main discrepancy between the two theoretical approaches occurs for the ^{13}C constant which is computed to have opposite signs in the two cases. This may be due to the different structural conformations found for the HPCPH and PhPCPPh radical cations. In fact, in planar allylic-type radicals, where the direct spin contribution vanishes, a negative hfs constant due to the spin polarisation is expected for the central atom, while upon rotation about the PC bonds the direct contribution should overcome the spin polarisation component.

In the radical anion the experimental hfs constants should be compared with those computed for both the *cis*- and *trans*-like conformations since the energy difference between the two conformers is small. In this case the ^{13}C constant computed for the *cis*-like ($a_{^{13}C}$ = 1.63 mT) and *trans*-like ($a_{^{13}C}$ = 1.40 mT) conformations are equally in accord with the experimental value determined both in the chemical and electrochemical reduction. On the other hand, the ^{31}P constant is significantly underestimated in the *cis*-like conformation ($a_{^{31}P}$ = 3.52 mT), the discrepancy with experiment largely decreasing in the *trans*-like conformation ($a_{^{31}P}$ = 5.01 mT), with a reasonably small deviation from the experimental value observed upon chemical reduction. Agreement slightly improves when the roto-inversion motion about the central carbon atom is taken into account ($\langle a_{^{31}P}\rangle$ = 5.17 and 5.26 mT at 193 and 298 K, respectively) since the ^{31}P hfs value increases significantly with increasing ω [$a_{^{31}P}(\omega = 180°)$ = 6.35 mT]. The discrepancy remains large if the theoretical ^{31}P hfs constant is compared with that measured in the radical upon electrochemical reduction. The effect of the roto-inversion motion is computed to be small for the ^{13}C constant ($\langle a_{^{13}C}\rangle$ = 1.44 and 1.47 mT at 193 and 298 K, respectively).

Since in the previous study on the HP=C=PH radical anion it was concluded that this species should rapidly interconvert between two equivalent asymmetric C_1 *trans*-like conformations, we have compared the hfs constants computed with the two different theoretical approaches for the *trans*-like conformation. The $a_{^{31}P}$ value computed for the PhPCPPh radical anion in the *trans*-like configuration is significantly smaller than that computed previously at the PMP2/6311+G** level for the unsubstituted HPCPH radical anion [7.64 mT, average value of the two unequivalent phosphorus atoms ($a_{^{31}P1} = 2.21$ mT, $a_{^{31}P2} = 13.06$ mT) in the C_1 symmetry]. The deviation is, however, much smaller if the symmetric C_2 conformation is considered ($a_{^{31}P} = 6.49$ mT). As found for the radical cation the hfs constant at the central carbon atom is computed to have opposite signs in the two theoretical studies. In this case the discrepancy can not be due to structural effects, the optimum value of the dihedral angle ω being similar in the unsubstituted and diphenyl substituted diphosphaallene radical anions. Hence, the observed discrepancy may be due either to the electronic effect of the phenyl rings or to the different theoretical approach employed in the two studies. We have computed the ^{13}C constant at the UB3LYP/6-311+G** level as well as at the more reliable UQCISD/6-311+G** level for the unsubstituted HPCPH radical anion at the geometry optimised previously at the UMP2/6-311+G** level.[6] Interestingly, the values computed at the UB3LYP ($a_{^{13}C} = 1.61$ mT) and UQCISD ($a_{^{13}C} = 1.73$ mT) levels are very similar to that computed at the UB3LYP/6-311G** level for the diphenyl diphosphaallene radical anion and have opposite sign to that computed previously from the projected UMP2 spin density ($a_{^{13}C} = -2.89$ mT). As a consequence, the magnetic properties of diphosphaallene radical ions obtained from the projected UMP2 spin density should be considered with extreme caution.

Optical transitions. The optical spectrum (transition wavelengths λ and oscillator strengths f) of the radical cation has been computed with the EOM-CCSD/POL method which was shown to reproduce well the UV–vis spectra of small molecules.[18] Such a calculation is not conceivable even for the diphenyl derivative owing to the large computational resources required by this approach, so the optical spectrum has been computed for the unsubstituted HPCPH radical cation constrained in the full *trans* conformation ($\omega = 180°$), *i.e.* in the more stable conformation adopted by the diphenyl derivative. The optical spectrum of the parent neutral compound has also been computed for comparison.

Table 4 shows that the theoretical results are in fairly good accord with experiment. More importantly, calculations predict for the radical cation a transition in the visible region ($\lambda > 400$ nm), while in the corresponding neutral molecule the longer wavelength transitions are computed to occur near 300 nm.

In particular, the calculations indicate that in the radical cation the lowest energy transition from the SOMO [allylic-type non-bonding $\pi_{nb}(b_g)$ MO localised on the phosphorus atoms] to the LUMO [$\sigma_C(b_u)$ MO] should not be detectable in our experimental conditions since it is predicted to occur in the near infrared region with very weak intensity. Calculations also suggest that the absorption in the visible region ($\lambda_{max} \approx 410$ nm) might be assigned to excitation from the SOMO to the second LUMO [antibonding $\pi^*(a_u)$ allylic-type MO]. The assignment of the second band ($\lambda_{max} = 315$ nm) is not straightforward: it extends to $\lambda < 300$ nm and its intensity appears to be greater than that shown by the first band. The calculations suggest that this broad band could probably originate from the overlapping of three transitions, the most intense of which is due to excitation of an electron with β spin from the doubly occupied $\pi(b_u)$ bonding MO to the SOMO, and the other two transitions mainly involve electron transfer in the σ plane from the P lone pair [$\sigma n_P(a_g)$ MO] to the 2pσ empty carbon atomic orbital [$\sigma_C(b_u)$ MO].

Table 4 Vertical optical transitions (wavelengths λ and oscillator strengths f) for HPCPH and its radical cation constrained in the full *trans* conformation computed at the EOM-CCSD/POL level along with experimental λ_{max} value for **1** and **4**

Symmetry	λ/nm	*f*	Exp/nm
		Neutral	
B	308	0.0054	
			275
A	300	0.0022	
A	264	0.0022	225
		Cation	
A_u	842	0.0002	
B_u	430	0.0112	405,[a] 410[b]
B_u	317	0.0055	
A_u	286	0.0125	320,[a] 315[b]
B_u	282	0.0068	

[a] In CH_2Cl_2. [b] In CCl_4.

In the neutral parent compound **1** the first intense absorption at 275 nm should include two transitions computed at *ca.* 300 nm. Thus, the total intensity is computed to be much greater than that for the transition predicted at shorter wavelength (264 nm) in accord with the CH_2Cl_2 experiment. Both bands are due to transitions from the nearly degenerate doubly occupied π-type MOs to the nearly degenerate antibonding π*-type MOs.

Discussion

For the sake of simplicity it is advisable to discuss the radical ions separately.

Radical cation

The cyclic voltammetric curves observed for the oxidation of **1** either in THF or CH_2Cl_2 are not well defined; yet there is little doubt that the oxidation potentials can not be lower than *ca.* 2.0 V *vs.* SCE. It is not possible to compare this value with that previously reported in the literature (1.5 V), because it was not stated with respect to which reference electrode the latter potential had been measured.[5]

The EPR spectra of **4** (or **4***) recorded in THF substantially agree with the earlier published data. Our calculations suggest that the radical cation adopts a sort of allylic-like structure and predict a phosphorus splitting very close to the experimentally measured value. On the other hand, the predicted ^{13}C splitting is about one half of the experimental value, this being possibly a consequence of approximating the tri-*tert*-butyl substituted phenyl groups to unsubstituted phenyl rings (see previous section). The lowest energy conformation should correspond to a full *trans* arrangement with a P^1–Ph^1, P^2–Ph^2 dihedral angle ($\omega = 180°$) significantly larger than that predicted by earlier MO calculations (*ca.* 135°).[5] A *cis*-like conformation is predicted to correspond to the second-lowest energy minimum, with a dihedral angle (46.8°) similar to that calculated previously.[5]

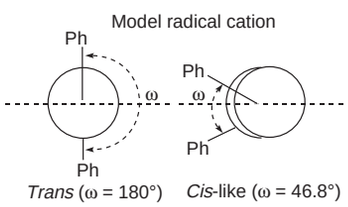

The dashed line represents the PCP plane

On the other hand, the EPR spectrum in hexafluoroisopropanol indicated additional coupling of the unpaired electron with the hydrogens of the two substituted aromatic rings, a feature not observed previously possibly because of the poorer resolution of the spectra in THF solution. Several sets of

parameters have been found to provide a satisfactory simulation of the hyperfine pattern exhibited by each individual line of the main triplet (quartet) in the experimental spectrum. Although good simulations were obtained assuming a π-like distribution of the spin density, it can not be excluded that only the *tert*-butyl groups in the *ortho*-positions of the aromatic rings undergo a through-space interaction with the unpaired electron. Actually, while the allylic-type orbital implies substantial spin density on the two phosphorus atoms, the two aromatic rings are almost perpendicular to the SOMO, that is in an arrangement favouring through-space interactions while preventing conjugative delocalisation. A rough estimate of the hydrogen couplings can be obtained by the AM1 method. Only the direct contribution due to the unpaired electron distribution in the SOMO has been evaluated using the restricted open approach since at the unrestricted level the spin contamination is too large ($S^2 = 1.57$). In the full-*trans* conformation the average value of the hydrogen couplings of the *tert*-butyl groups is 0.071 mT in the *ortho*-position and essentially null in the *para*-position. Interestingly, while a small rotation (10°) of the phenyl groups about the orthogonal conformation does not modify significantly the average value (0.067 mT), this is lowered to 0.045 mT for larger rotations (30°). The coupling of the *meta* protons is computed to be 0.049 mT, but the spin polarisation contribution could significantly modify this value. Thus, these semiempirical calculations suggest that the observed hyperfine pattern should be due to through-space delocalisation of the unpaired electron to the 36 hydrogens of the *tert*-butyl groups in the *ortho*-position and, possibly, to through bond delocalisation to the 4 *meta* hydrogens.

The EPR experiments in methylene chloride deserve a special comment. Indeed the EPR spectra observed upon oxidation of **1** (or **1***) indicate the simultaneous presence of two radicals **4** and **5** (**4*** and **5***), characterised by very similar spectral parameters, which are both in line with those expected for the radical cation. In principle the spectra might be attributed to the *trans* and *cis* isomers of **4** corresponding to the two energy minima predicted by calculations. Such an assignment would however contrast with the observation of a single radical species upon oxidation of **1** (or **1***) in THF as well as in hexafluoroisopropanol, and with the fact that the *trans* conformer is predicted to be by far more populated than the *cis*. The possibility that one of the radicals originates from an impurity is rather unlikely in view of the fact that the two species are present in the same amount and are characterised by the same spectral parameters when working with either **1** or **1***, which have been synthesised *via* two independent routes. The further possibility that one of the radicals is an adventitious species resulting from a reaction between the initially formed radical cation **4** (or **4***) and the solvent must also be considered, although it appears unlikely in view of the fact that their relative amounts do not vary with time and with the initial concentration of the substrate. Besides, the nature of the paramagnetic species **5** which would be formed through any such reaction is rather obscure as its EPR spectral parameters are not substantially modified with respect to those exhibited by **4**. We therefore suggest that the spectra observed in CH_2Cl_2 are due to the radical cation **4** and to its "solvated" form **5**, or, better, to a complex between the radical cation and a solvent molecule, formed possibly through coordination of the two phosphorus atoms of **4** by the chlorine atoms of a CH_2Cl_2 molecule.

The time evolution of the absorption at 320 and 405 nm characterising the UV–vis absorption spectrum of radical cation **4** in methylene chloride is consistent with the two step process outlined in eqns. (3) and (4).

$$CHCl_2^{\bullet} + \mathbf{1} \longrightarrow \underset{\mathbf{11}}{[\mathbf{1}^{\delta+} \cdots CHCl_2^{\delta-}]^{\bullet}} \qquad (3)$$

$$\underset{\mathbf{11}}{[\mathbf{1}^{\delta+} \cdots CHCl_2^{\delta-}]^{\bullet}} \longrightarrow \mathbf{4} + CHCl_2^{-} \qquad (4)$$

In the first step the dichloromethyl radical attacks the P=C=P double bond system causing the formation of a dipolar intermediate **11**. In fact, this first process is a pseudo-first order reaction, due to the excess of **1** with respect to the oxidising radicals, and proceeds with a rate close to the diffusional limit ($k_3 = 6.36 \times 10^9$ dm^3 mol^{-1} s^{-1}). The second and slower process ($k_4 = 7.21 \times 10^4$ s^{-1}) is identified as the definite intramolecular exchange of an electron between the two components of the dipole.

The time evolution of the similar UV–vis absorption spectrum observed in carbon tetrachloride can be interpreted as the occurrence of a simple outer-sphere electron transfer process between trichloromethyl radicals and **1**, also occurring at a nearly diffusion controlled rate ($k_5 = 5.64 \times 10^9$ dm^3 mol^{-1} s^{-1}).

$$CCl_3^{\bullet} + \mathbf{1} \longrightarrow \mathbf{4} + CCl_3^{-} \qquad (5)$$

The intensity ratio between the two peaks at 315 and 410 nm in CCl_4 is reversed with respect to that observed in CH_2Cl_2. This observation is in line with the fact that the intermediate adduct **11**, as charge transfer complexes usually do, contains the same bands of the two incipient ions, differing only in intensity. While in CH_2Cl_2 the 405 nm peak of the adduct bleaches as the charge separation proceeds, and simultaneously the peak at 320 nm of **4** becomes more and more intense, in CCl_4 both bands grow in parallel and are fully developed in 9 μs. We therefore believe that in the latter case their intensity ratio is more likely to represent the probability ratio of the two electronic transitions in the radical cation **4**.

Ab initio calculations carried out on the HPCPH simplified model suggest that these absorption bands should be attributed to π→SOMO and SOMO→second LUMO transitions for which λ_{max} values of *ca.* 290 and 430 nm are predicted. The higher wavelength absorption is also predicted to be the less intense of the two. In agreement with experiment, these calculations exclude any absorption by **1** beyond *ca.* 310 nm.

As reaction (5) is assumed to be an outer-sphere electron transfer (ET) process, it should be possible to use Marcus theory to evaluate the corresponding rate constant in order to compare it with the experimental value. A fundamental prerequisite in this respect is the knowledge of the standard free energy change ΔG° for reaction (5), which can be evaluated (in kcal mol^{-1}) from eqn. (6), where $E^{\circ}_{CCl_3^{\bullet}/CCl_3^{-}}$ and $E^{\circ}_{4/1}$ are

$$\Delta G^{\circ} = -23.06[E^{\circ}_{CCl_3^{\bullet}/CCl_3^{-}} - E^{\circ}_{4/1}] \qquad (6)$$

the standard reduction potentials of the appropriate redox couples. While the value of $E^{\circ}_{4/1}$ is known from the electrochemical experiments described above ($E_{1/2}$ is considered equal to E° within the usual assumptions) although in a solvent different from that in which k_5 has been determined, the value of $E^{\circ}_{CCl_3^{\bullet}/CCl_3^{-}}$ is not available. On the other hand, Marcus theory can be used in order to obtain an approximate estimate of $E^{\circ}_{CCl_3^{\bullet}/CCl_3^{-}}$ from the experimentally determined rate constant k_5. As a matter of fact, by utilising this theory (see Appendix) the resulting standard potential $E^{\circ}_{CCl_3^{\bullet}/CCl_3^{-}}$ in CCl_4 is estimated in the range 1.6–1.3 V *vs.* SCE.

Radical anion

The reduction cvc's exhibit two reduction peaks with an $E_{1/2}$ difference of *ca.* 500 mV; their characteristics suggest that the electrons are strongly interacting, the extent of the interaction being typical of the coupling of two electrons in the same redox orbital. In view of the fact that the interactions between two electrons introduced in the two phenyl groups should be small, the two redox processes should be essentially centred in a molecular orbital for which the highest charge density is located in the central part of the molecule, *i.e.* the PCP fragment. This is substantiated by the results of theoretical calculations

performed on the dianionic species at the B3LYP/6-311G** level which predict for this species a full *trans* conformation ($\omega = 180°$) with the two extra electrons located in the same σ MO. The paramagnetic dianion (triplet state) lies 1.0 eV higher in energy. In turn, the diamagnetic dianion is computed to be 3.1 eV less stable than the radical anion. This value is much greater than that found experimentally (*ca.* 0.5 eV). However the simple Born theory[19] predicts that the interaction with solvent should stabilise the dianion species with respect to the radical anion by 1.9 and 2.1 eV in THF and ACN respectively. The radius of the diphenyl derivative has been employed in the calculation since it is intermediate between those of the unsubstituted and bis(2,4,6-tri-*tert*-butylphenyl) derivatives so as to simulate the actual distribution of the molecules of solvent around the negatively charged species. Thus, taking into account solvation, the instability of the dianion with respect to the radical anion decreases to about 1.0 eV, *i.e.* in better accord with experiment.

As already mentioned, in our hands the EPR spectra obtained by reduction of **1** (and **1***) proved much more complex than previously reported,[6] and their rather intriguing discussion requires that at least three different hypotheses be considered.

A first possibility is that the observed spectra result from the overlapping of the signal due to the radical anion **6** (or **6***), a broad "normal" 1:2:1 triplet (triplet of doublets), with a narrower doublet (doublet of doublets) of multiplets. In this case the reversible disappearance and reappearance of the outer lines on lowering and raising the temperature would imply the existence of an equilibrium between the radical and a diamagnetic species (a dimer?), shifted in favour of the radical at higher temperatures, a feature more characteristic of neutral free radicals than of radical anions. It is however hard to propose a structure for the radical responsible for the sharper central signal, the only clear point being that it should still contain the central carbon atom of the starting compound(s), as indicated by the variation of the spectral pattern on isotopic substitution. Besides, it seems at least odd that in the radicals from the ^{13}C enriched derivative the ^{13}C splitting of the central signal is the same as that of the outer lines. Anyway, even if this were the case, the phosphorus splittings would be sizeably larger than that computed for both the *cis*-like and *trans*-like conformations and also larger than the maximum value (6.32 mT) computed for the full *trans* conformation which, however, lies 2.9 kcal mol^{-1} higher in energy. Furthermore, calculations suggest that both conformers should be detectable.

A second hypothesis, apparently in line with the previous report,[6] is that all the observed lines belong to the same spectrum, and that the unusual spectral pattern reflects dipolar broadening of the lines associated with the triplet state of the two equivalent phosphorus nuclei, similarly to what was observed previously for the radical cation of a diaryl diphosphine[20,21] or for 1,1-difluorobenzyl radical.[22] In this case, however, it seems difficult rationalising the hyperfine structure exhibited by the central group under higher resolution conditions. Actually, the best fitting (in fact a very good one) between the experimental and the computer simulated traces was obtained by assuming that the unpaired electron, besides interacting with the two ^{31}P and the ^{13}C (when present) nuclei, is also coupled with two sets of nine equivalent hydrogens (0.047 and 0.082 mT, respectively) and a single hydrogen (0.328 mT). Although the ^{31}P and ^{13}C hfs constants are reasonably consistent with previous values attributed to the radical anion **6** (or **6***),[6] a justification of the additional hyperfine pattern would require the interaction of the unpaired electron with only one aromatic ring which, in addition, should be blocked in such a way that only one of the *meta* hydrogens and only two out of the three *tert*-butyl groups exhibit an hyperfine coupling. Such a set up should lead, in contrast with experiment, to the observation of two unequivalent phosphorus splittings. Actually the 0.328 mT doublet cannot originate from two unequivalent phosphorus couplings, because in this case all the spectral lines should exhibit a normal intensity.

All the above points seem to cast serious doubts on the attribution of the observed spectrum to the radical anion **6** (or **6***), yet the disconcerting observation that the electrolytic reduction of the 3,3-dichloro-1,2-diphosphirane **8** (or **8***) affords the same spectrum detected with **1** (or **1***) might instead be viewed as lending further support to this identification. Compound **8** is in fact converted to the diphosphaallene **1** by reaction with methyllithium in THF,[1] and it is possible that, as outlined in Scheme 4, the electrochemical process is actually a mimic of the synthetic reaction.

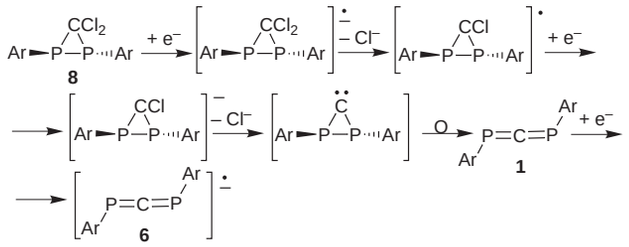

Scheme 4

Also for this second hypothesis, agreement with MO calculations is very poor. In addition to the already discussed discrepancy in the phosphorus hfs constant, the *meta* hydrogen splittings are computed to be much smaller (<0.07 mT, in particular 0.01 and 0.05 mT in the *cis*-like conformer, and 0.01 and 0.06 mT in the *trans*-like conformers), than the doublet experimentally observed (0.328 mT). Furthermore, AM1 calculations show that the spin density at any hydrogen of the *tert*-butyl groups is much smaller than that at *meta* hydrogens, thus suggesting that a hydrogen of the *tert*-butyl groups can not be responsible for the observed doublet.

In this context, the increase of the EPR spectral intensity detected after interrupting the electrochemical reduction of either **1** or **8** should also be considered. In principle this might be viewed as a consequence of the experimental set-up, our EPR electrolytic cells only having a working electrode and a counter electrode, but no reference electrode. The consequent impossibility of achieving exact control of the working electrode potential could lead to the formation of substantial amounts of the dianion **7** at the expense of the radical anion **6**. Upon interruption of the current, a comproportionation might take place between the dianion and compound **1** to form the radical anion **6**. It should however be recalled that the rates of decomposition of the dianion **7** and of the radical anion **6** have been determined as 8×10^2 and 3×10^2 s^{-1}, respectively; this is in contrast with the fact that the spectra can be observed over a long time interval after the electrolysis interruption.

The third possibility stems from the EPR spectra observed by chemical reduction. Whether or not the spectra observed at room temperature are due to the radical anion, those recorded at low temperature by reduction of **1** with the Na–K alloy in the presence of a crown ether should be due to an ion pair **10** (see Table 1) between the radical anion and an alkali counterion, the latter being externally complexed by the crown ether. The additional doublet splitting observed when replacing **1** with the isotopically marked **1*** would also be consistent with this assignment. The normal 1:2:1 shape of the triplet spectral pattern should be attributed to a different conformational preference of the ion pair with respect to the free anion, also reflected in the different values of the hfs constants measured for the two species. On the basis of MO calculations performed previously[6] on the unsubstituted radical anion this would mean that the ion pair is locked in the symmetric C_2 structure ($a_{^{31}P} = 6.49$ mT), while the free anion inverts rapidly between two equivalent asymmetric C_1 structures (average $a_{^{31}P}$ value = 7.64 mT). Although the agreement with experiment ($a_{^{31}P} = 6.2$ and 7.68

mT, respectively) would be very good, the present calculations indicate that this agreement is fortuitous. They confirm that this radical anion has to be considered as a fluxional system due to the *quasi* linearity of the PCP linkage: the C_1 structure lies only 0.1 kcal mol^{-1} higher in energy above the symmetric C_2 structure but the average value of the ^{31}P constants ($a_{^{31}P}$ = 5.05 mT, $a_{^{31}P1}$ = 4.33 mT and $a_{^{31}P2}$ = 5.77 mT) increases little with respect to that computed for the C_2 structure ($a_{^{31}P}$ = 5.01 mT). The optimum values of the torsion angles in the asymmetric structure ($C^{Ph1}P^1CP^2$ = 60.4°, $C^{Ph2}P^2CP^1$ = 161.3°) determined at the UB3LYP/6311G** level are similar to those found previously for the unsubstituted HPCPH radical anion at the UB3LYP/6-31+G** level ($H^1P^1CP^2$ = 60.2°, $H^2P^2CP^1$ = 157.2°). Furthermore, while we recall that the hfs constants computed from projected UMP2 spin density should be considered with caution, we emphasise the good agreement between the ^{31}P and ^{13}C hfs constants calculated for **6*** in the *trans*-like conformation and those we experimentally measured. According to these calculations, the relatively large phosphorus splitting is due to the positive contribution to the s spin density from the 3s component of the phosphorus lone pairs in the SOMO (σ), a contribution which is absent in the π-type radical cation **4**.

Calculations predict that also for the radical anion a *trans* and a *cis* conformation correspond to an absolute and a relative energy minimum, the dihedral P^1–Ph^1,P^2–Ph^2 angle for the *trans* conformer being lower than in the corresponding conformer of the radical cation. The energy difference between the two conformers is computed to be small so that both species should be detectable in the free anion. In the ion pair the *trans*-like structure could be largely preferred since there is a much larger space to allocate the counterion complexed with the crown ether.

We therefore believe that the spectra observed on Na–K reduction of **1** and **1*** can be safely attributed to the corresponding radical ion pairs **10** and **10***, despite a previous statement that ". . . *electrochemical and chemical reductions of* ***1*** *lead to EPR spectra exhibiting the same hyperfine structure . . .*".[6] In this respect, the observation of a hyperfine splitting from the metallic counterion would have been useful for an unambiguous identification of the ion pair. In the present case the non-observation of a metal splitting is not surprising in view of the presence of dibenzo-18-crown-6 ether, and it is unfortunate that experiments carried out with different crown ethers or without a crown ether altogether did not result in the observation of any spectrum at low temperature, and afforded the spectrum of radical **9** at higher temperatures (T > 0 °C).

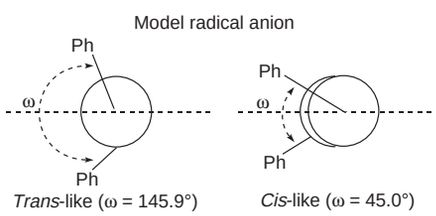

The dashed line represents the PCP plane

On the other hand, the observed thermal lability of these species is consistent with the results of the CV experiments which show that the first reduction peak, corresponding to the formation of the radical anion, is reversible at low temperature but becomes irreversible as the temperature is substantially raised. In this light we are also dubious about the identification of the radical anion **6** (**6***) as the species responsible for the EPR spectrum detected upon electrolytic reduction of **1** (or **1***) at room temperature, the intriguing complexity of the high resolution spectra casting further doubts on this assignment.

The reduction of **1** with lithium was instead in line with the previous report,[6] and the failure in detecting spectra similar to those observed upon Na–K reduction when using lithium as reducing agent either in the absence or in the presence of a suitable crown ether is in our opinion a consequence of the different experimental conditions. Actually, lithium was used combined with mercury in order to have a wider and cleaner contact surface, but the amalgam reacted with **1** only above −40 to −30 °C,‡ leading under these conditions to the observation of spectra identical to those observed in the electrolytic experiments and not consistent with the radical anion of **1**.

As a concluding remark, we wish to point out that while the diphosphaallene H–P=C=P–H certainly is an inadequate, oversimplified model to calculate the magnetic and structural properties of the radical ions, it proves adequate to predict the electronic properties (optical transitions) of the title compound and the corresponding radical cation under the constraint that for the latter the geometry optimised for Ph–P=C=P–Ph is used. This reflects the fact that the optical transitions essentially involve the P=C=P moiety of the molecule.

Experimental

The normal and 2-^{13}C labelled bis(2,4,6-tri-*tert*-butylphenyl)-1,3-diphosphaallenes **1** and **1*** were synthesised according to described procedures.[4] All other chemicals were commercially available, as were the solvents which were used after dehydration by standard methods.

Cyclic voltammetry

Tetraethylammonium tetrafluoroborate (TEATFB) or tetrabutylammonium hexafluorophosphate (TBAHFP), puriss. from Fluka, were employed as supporting electrolytes and used as received. ACN (UVASOL, Merck), THF (LiChrosolv, Merck) purified as previously described,[23] and CH_2Cl_2 (Fluka) were distilled into the electrochemical cell prior to use, using a trap-to-trap procedure. The other solvents were transferred under argon from the original air-tight containers into a Schlenk flask containing activated 4 Å molecular sieves and kept under vacuum until use.

The one-compartment airtight electrochemical cell had high-vacuum glass stopcocks fitted with either Teflon or Kalrez (DuPont) O-rings in order to prevent contamination by grease. The connections to the high-vacuum line and to the Schlenk flask containing the solvent were obtained by spherical joints also fitted with Kalrez O-rings. The pressure in the electrochemical cell prior to the trap-to-trap distillation of the solvent was typically 2.0–3.0 × 10^{-5} mbar. The working electrode consisted of a platinum disc ultramicroelectrode (Goodfellow, 10 μm diameter) sealed in glass, the counter electrode was a platinum spiral, and the quasi-reference electrode was a silver spiral whose drift was negligible for the time required for a single experiment. Both the counter and the reference electrode were separated from the working electrode by *ca.* 0.5 cm. Potentials were measured with the ferrocene standard and are always referred to SCE.[24] $E_{1/2}$ values correspond to ($E_{p,c}$ + $E_{p,a}$)/2 from CV curves. Ferrocene was also used as internal standard for checking the electrochemical reversibility of a redox couple.

The number of electrons corresponding to an electrochemical process was determined by comparison to ferrocene, and, independently, from the value of the limiting current $i_{lim} = 4nFDca$ (where n is the number of electrons, c the concentration and a the radius of the UME) at a disc ultramicroelectrode (a = 12.5 μm), the diffusion coefficient value D having been obtained from a chronoamperometric experiment performed at the same electrode. By monitoring i over a time window embracing the transient and the steady state regions, i_{lim} was obtained while D could be determined from the slope of the plot of $i(t)/i_{lim}$ *vs.* $t^{-1/2}$.[25]

‡ Below this temperature only a narrow single line with $g = 2.0022_1$ was observed, probably due to solvated electrons.

Voltammograms were recorded with a custom-made high-gain potentiostat[26] controlled by either an AMEL Mod. 568 programmable function generator or an ELCHEMA Model FG 206 F, an AMEL Mod. 865 A/D converter, a Hewlett-Packard 7475A digital plotter and a Nicolet Mod. 3091 digital oscilloscope. Minimisation of the uncompensated resistance effect in the voltammetric measurements was achieved by the positive-feedback circuit of the potentiostat. The DigiSim 2.1 software by Bioanalytical Systems was used for the simulation of the CV curves.

EPR Experiments

Spectra were recorded on an upgraded Bruker ER200D X-band spectrometer, equipped with a dedicated data system, a variable temperature device, an NMR Gaussmeter for field calibration, and a frequency counter for the determination of *g*-factors. The latter were calibrated with respect to that of the perylene radical cation in conc. sulfuric acid.

Chemical oxidation was carried out in a fused silica sample tube (id = 1 mm) by adding a small amount of iodosobenzene bis(trifluoroacetate) to an argon purged solution of either **1** or **1*** in 1,1,1,3,3,3-hexafluoropropan-2-ol (HFP). Chemical reduction was carried out at low temperature in a vacuum-sealed Pyrex tube by passing over a sodium–potassium mirror a THF solution of either **1** or **1*** to which some dibenzo-18-crown-6 ether had been added.

Combined electrochemical–EPR experiments were performed at room temperature directly inside the spectrometer cavity using a 0.15 mm thick flat cell with a platinum gauze and a mercury pool or a platinum wire as electrodes, and operated through an AMEL 2051 general-purpose potentiostat. Oxidations were carried out in methylene chloride or THF, reductions in THF or DMF, using tetrabutylammonium perchlorate or tetrabutylammonium tetrafluoroborate as electrolytes (*ca.* 10^{-1} M).

Pulse radiolysis

Methylene chloride (Merck *pro analysis*) was treated as previously described. Purging of oxygen was achieved by saturating the solution with argon. Pulse radiolysis with optical detection was performed by using a 12 MeV electron linear accelerator (Linac).[27,28] The radiation dose per pulse (10–50 ns) was monitored by means of a charge collector plate placed behind the irradiation cell and calibrated with an O_2 saturated aqueous solution containing 0.1 M KSCN and by taking $G \times \varepsilon_{500\ nm} = 2.15 \times 10^4$ (100 eV)$^{-1}$ mol^{-1} dm^3 cm^{-1}. This dose was then corrected for the different electron density of the individual chloromethane with respect to water. 1 Gray (Gy) of irradiation dose corresponds to an absorbed energy of 1 J kg^{-1}. Spectral data were normalised to the same dose per pulse. The optical detection system employed the R955 Hamamatsu side-on photomultiplier and a double grating monochromator with 5 nm bandwidth (±2.5 nm) throughout the spectral measurements. Absorbance sensitivity was of the order of 1×10^{-3}. A remote controlled shutter limited the exposure of the samples to any effect of the analysing light. All the irradiations were made at room temperature in Spectrosil® cells 2 cm long and samples were renewed after each pulse. The electron beam was adjusted to the same shape and size as the cell by means of focusing magnets. Transient waveforms were captured by a Tektronix Transient Digitizer 7912AD and then processed with PC software for spectral and kinetic analysis.[29] The rise time was *ca.* 2 ns. Pre-irradiation spectra were checked by means of a Hewlett-Packard 8452A diode array spectrophotometer.

MO Calculations

Calculations have been carried out on the diphenyl-1,3-diphosphaallene and on its radical ions with the B3LYP method employing a valence triple-ζ basis set supplemented with polarisation functions, *p*-functions on hydrogens and *d*-functions on heavy atoms (6-311G(d,p)),[30–32] using the GAUSSIAN94 system of programs.[33] In this method, which is based on the Density Functional Theory, the exchange functional is a linear combination of Hartree–Fock, local, and gradient-corrected exchange terms (B3)[34] and the correlation functional is a non local gradient-corrected term (LYP).[35] Geometries have been optimised using an analytical gradient technique and hyperfine coupling constants have been evaluated as expectation values from the computed spin density matrices. Preliminary calculations on the radical anion have also been carried out augmenting the basis set with diffuse *s*- and *p*-functions on heavy atoms (6-311+G(d,p)).[36] On the highly symmetric linear full *trans* conformation the magnetic properties change little on adding diffuse functions on heavy atoms, the ^{13}C and ^{31}P constants being computed to be 2.32 and 6.35 mT, respectively, at the UB3LYP/6-311G** level and 2.29 and 6.23 mT at the UB3LYP/6-311+G** level. Thus, diffuse functions are not included in the calculations to save computational time.

Hfs constants for the radical anion in the *trans*-like conformation have been averaged over the thermally populated states of the roto-inversion mode which has been approximated with a one dimensional double-minimum potential:

$$V(\delta) = k\delta^2/2 + b\delta^4/2 + v\exp(-c\delta^2)$$

The Hamiltonian has been set up in the basis of the eigenfunctions of the harmonic oscillator[37] using a reduced mass $\mu = 3.7810^{-37}$ g cm^2. The values of the potential energy parameters ($k = 0.0158$ au rad^{-2}, $b = 0.057$ au rad^{-4}, $v = 0.0069$ au, $c = 18.2$ rad^{-2}) have been determined from a best fitting of the roto-inversion energy computed varying δ from 0 to 45° at 5° intervals and the hfs constants have been expanded in an even-power series of δ using a polynomial of 14th degree.

Geometries and energies have been also computed for the unsubstituted derivatives with the unrestricted quadratic configuration interaction method with single and double substitutions (UQCISD)[38] employing the same basis set. In this case hfs constants have been evaluated from generalised density matrices computed with the Z-vector method.[39] Optical transitions have been computed on the unsubstituted radical cation with the equation of motion coupled cluster method with single and double substitutions (EOM-CCSD)[40] using the ACES II program.[41] The polarised basis set (POL)[42,43] developed by Sadlej for high-level-correlated calculations of molecular electric properties has been employed in these calculations. This is a triple-ζ basis set with sufficient diffuse character to describe both Rydberg and valence excited states augmented with two sets of polarisation functions.

Acknowledgements

This work was partly supported by Ministero dell'Università e della Ricerca Scientifica e Tecnologica - MURST (Rome), by Consiglio Nazionale delle Ricerche (Rome) and by the University of Bologna (Funds for Selected Research Topics). The financial contribution from the Progetto Strategico Modellistica Computazionale di Sistemi Molecolari Complessi (CNR) is also acknowledged.

Appendix — Estimate of $E^\circ_{CCl_3^\cdot/CCl_3^-}$ by means of Marcus theory

In order to obtain an approximate estimate of the as yet unknown $E_{CCl_3^\cdot/CCl_3^-}$ value from the experimentally measured k_5, Marcus theory was used. Since $k_5 < 0.1\ k_d$ (the diffusional rate constant for the formation of precursor complex), the Marcus equation can be written in a simple version[44] as eqn. (7),

$$k_{el} = Z \exp\{-[(\lambda/4)(1 + \Delta G^{\circ\prime}/\lambda)^2/RT]\} \quad (7)$$

where k_{el} is the rate constant of the electron transfer reaction, $Z = 10^{11}$ M^{-1} s^{-1} is the pre-exponential factor (adiabatic ET), λ is the reorganisation energy, and $\Delta G^{\circ\prime}$ is the corrected free energy change of the reaction. The reorganisation energy consists of inner-sphere, λ_i, and outer-sphere, λ_o, terms. Assuming that the configuration changes of both reactants are sufficiently small, λ_i can be neglected, and the outer-sphere reorganisation energy, which arises mainly from solvation, can be evaluated from eqn. (8),[44] where $r_1 = 2$ Å and $r_2 = 8$ Å are the radii of CCl_3

$$\lambda_o = 331.2\ [(1/2r_1) + (1/2r_2) - (1/r_{12})][(1/n^2) - (1/\varepsilon)] \quad (8)$$

and **1**, respectively, approximated as hard spheres, and $r_{12} = r_1 + r_2$. The refraction index $n = 1.459$ and the relative permittivity (formerly known as dielectric constant) $\varepsilon = 2.24$ are the values for the present solvent (CCl_4) at 25 °C. A value of 1.64 kcal mol^{-1} is calculated for λ_o from eqn. (8), and by introducing this value for λ_o and the experimental value for k_5 in equation 9, obtained by rearranging eqn. (7), a value of 1.70 kcal mol^{-1} was obtained for $\Delta G^{\circ\prime}$.

$$\Delta G^{\circ\prime} = \lambda\{[(RT\ln(Z/k_{el})/(\lambda/4)]^{1/2} - 1\} \quad (9)$$

By correcting $\Delta G^{\circ\prime}$ for the electrostatic free energy change A upon ET in the transition state, using eqn. (10) and (11),

$$\Delta G^{\circ\prime} = \Delta G^{\circ} + A \quad (10)$$

$$A = (331.2/(\varepsilon r_{12}))f(Z_1 - Z_2 - 1) \quad (11)$$

where Z_1 and Z_2 are the charges of the acceptor and donor respectively (0 for both), $f = 1$ (*i.e.* zero ionic strength), a value of 16.48 kcal mol^{-1} is obtained for ΔG°. In order to evaluate $E^{\circ}_{CCl_3^{\cdot}/CCl_3^-}$ in CCl_4, knowing ΔG°, it is necessary to introduce in eqn. (4) the value of $E^{\circ}_{4/1}$ determined in the same solvent. We are now facing the problem of converting data valid for one solvent to values for another solvent. One simple hypothesis is that the variation of redox potentials by changing the solvent can be accounted for by the dielectric continuum Born model[19] according to which the variation in $E_{1/2}$ for the redox couple **4/1**, upon switching from CH_2Cl_2 to CCl_4, is given by eqn. (12),

$$\Delta E_{1/2} = (1/F)\{(331.2/2)\ [(1/\varepsilon_{CCl_4}) - (1/\varepsilon_{CH_2Cl_2})]\}(1/r_4) \quad (12)$$

where F is the Faraday constant (23.07 kcal V^{-1} mol^{-1}), $r_4 = 8$ Å is the radius of the species formed and the other symbols have the same meaning as defined above. The use of eqn. (12) gives for $\Delta E_{1/2}$ the value of 0.3 V, so that from the experimental value of 1.97 V for $E_{1/2,4/1}$, determined in CH_2Cl_2, an estimated value of 2.27 V is obtained for $E_{1/2,4/1}$ in CCl_4. Inserting this value into eqn. (6), along with the estimated value of 16.48 kcal mol^{-1} for ΔG°, the value of 1.56 V is obtained for $E^{\circ}_{CCl_3^{\cdot}/CCl_3^-}$. If instead the value of 1.97 V, uncorrected for the change of the solvent, is used $E^{\circ}_{CCl_3^{\cdot}/CCl_3^-}$ is evaluated as 1.26 V.

On the basis of the above treatment, in spite of the severity of the approximations made, it can be deduced that the as yet unknown value for $E^{\circ}_{CCl_3^{\cdot}/CCl_3^-}$ should not differ much from 1.45 V *vs*. SCE, the midpoint potential of the range 1.6 − 1.3 V *vs*. SCE.

References

1 M. Yoshifuji, K. Toyota and N. Inamoto, *J. Chem. Soc., Chem. Commun.*, 1984, 689; H. H. Karsch, F. H. Köhler and H.-U. Reisacher, *Tetrahedron Lett.*, 1984, 3687; R. Appel, P. Fölling, B. Josten, M. Siray, V. Winkhaus and F. Knoch, *Angew. Chem., Int. Ed. Engl.*, 1984, **23**, 619.
2 H. H. Karsch, H.-U. Reisacher and G. Müller, *Angew. Chem., Int. Ed. Engl.*, 1984, **23**, 618.
3 M. T. Nguyen and A. F. Hegarty, *J. Chem. Soc., Perkin Trans. 2*, 1985, 2005; N. J. Fitzpatrick, D. F. Brougham, P. J. Groarke and M. T. Nguyen, *Chem. Ber.*, 1994, **127**, 969.
4 A. Alberti, M. Benaglia, M. A. Della Bona, M. Guerra, A. Hudson and D. Macciantelli, *Res. Chem. Intermed.*, 1996, **22**, 381.
5 M. Chentit, H. Sidorenkova, A. Jouaiti, G. Terron, M. Geoffroy and Y. Ellinger, *J. Chem. Soc., Perkin Trans. 2*, 1997, 921.
6 H. Sidorenkova, M. Chentit, A. Jouaiti, G. Terron, M. Geoffroy and Y. Ellinger, *J. Chem. Soc., Perkin Trans. 2*, 1998, 71.
7 L. Eberson, M. Hartshorn, O. Persson and F. Radner, *J. Chem. Soc., Chem. Commun.*, 1996, 2105.
8 H. B. Stegmann and K. Scheffler, *Angew. Chem.*, 1964, **76**, 610; R. Biehl, M. Plato and K. Moebius, *J. Chem. Phys.*, 1975, **63**, 3515.
9 J. Smid, in *Ions and Ion Pairs in Organic Reactions*, M. Szwarc, ed., Wiley, New York, 1972, vol. 1.
10 S. S. Emmi, G. Beggiato and G. Casalbore-Miceli, *Radiat. Phys. Chem.*, 1989, **33**, 29.
11 Z. B. Alfassi, S. Mosseri and P. Neta, *J. Phys. Chem.*, 1989 **93**, 1380.
12 A. Hummel, in *Advances in Radiation Chemistry*, M. Burton and J. L. Magee eds., Wiley, New York, 1974.
13 M. Guerra, *Pure Appl. Chem.*, 1995, **67**, 797.
14 M. Guerra, *J. Phys. Chem.*, 1996, **100**, 19 356.
15 V. Barone, *J. Chem. Phys.*, 1994, **101**, 6834.
16 J. W. Gauld, L. A. Eriksson and L. Radom, *J. Phys. Chem.*, 1997, **101**, 1352.
17 M. Guerra, *J. Am. Chem. Soc.*, 1992, **114**, 2077.
18 J. E. Del Bene, J. D. Watts and R. J. Bartlett, *Chem. Phys. Lett.*, 1995, **246**, 541.
19 J. O'M. Bockis and A. K. N. Reddy, in *Modern Electrochemistry*, vol. 1, ch. 2. 2, Plenum Press, New York, 1970.
20 M. Culcasi, G. Gronchi and P. Tordo, *J. Am. Chem. Soc.*, 1986, **107**, 7191.
21 Y. Ayant, N. Kernevez, A. Thevand, L. G. Werbelow, M. Culcasi, G. Gronchi and P. Tordo, *J. Magn. Res.*, 1986, **70**, 446.
22 J. Cooper, A. Hudson, R. A. Jackson and M. Townson, *Mol. Phys.*, 1972, **23**, 1155.
23 F. Paolucci, M. Marcaccio, S. Roffia, G. Orlandi, F. Zerbetto, M. Prato, M. Maggini and G. Scorrano, *J. Am. Chem. Soc.*, 1995, **117**, 6572.
24 S. Roffia, R. Casadei, F. Paolucci, C. Paradisi, C. A. Bignozzi and F. Scandola, *J. Electroanal. Chem.*, 1991, **302**, 157.
25 P. Ceroni, F. Paolucci, C. Paradisi, A. Juris, S. Roffia, S. Serroni, S. Campagna and A. J. Bard, *J. Am. Chem. Soc.*, 1998, **120**, 5480 and references therein.
26 C. Amatore, A. Jutand and F. Pflüger, *J. Electroanal. Chem.*, 1987, **218**, 361.
27 A. Hutton, G. Roffi and A. Martelli, *Quad. Area Ric. Emilia-Romagna*,, 1974, **5**, 67.
28 A. Martelli, S. S. Emmi, N. Camaioni, A. Monti and S. Draghi, in *Proceedings V National Meeting SIRR*, Rome, 1989, 291.
29 N. Camaioni, S. S. Emmi and Q. Mulazzani, *FRAE Report N. 9*, 1993.
30 R. Krishnan, J. S. Binkley, R. Seeger and J. A. Pople, *J. Chem. Phys.*, 1980, **72**, 650.
31 A. D. McLean and G. S. Chandler, *J. Chem. Phys.*, 1980, **72**, 5639.
32 M. J. Frisch, J. A. Pople and J. S. Binkley, *J. Chem. Phys.*, 1984, **80**, 3265.
33 M. J. Frisch, G. W. Trucks, H. B. Schlegel, P. M. W. Gill, B. G. Johnson, M. A. Robb, J. R. Cheeseman, T. A. Keith, G. A. Petterson, J. A. Montgomery, K. Raghavachari, M. A. Al-Laham, V. G. Zakrzewski, J. V. Ortiz, J. B. Foresman, J. Cioslowski, B. B. Stefanov, A. Nanayakkara, M. Challacombe, C. Y. Peng, P. Y. Ayala, W. Chen, M. W. Wong, J. L. Andres, E. S. Replogle, R. Gomperts, R. L. Martin, D. J. Fox, J. S. Binkley, D. J. Defrees, J. Baker, J. J. P. Stewart, M. Head-Gordon, C. Gonzalez and J. A. Pople, GAUSSIAN94, Revision C, Gaussian, Inc., Pittsburgh, PA, 1995.
34 A. D. Becke, *J. Chem. Phys.*, 1993, **98**, 5648.
35 C. Lee, W. Yang and R. G. Parr, *Phys. Rev. B*, 1988, **37**, 785.
36 T. Clark, J. Chandrasekhar, G. W. Spitznagel and P. v. R. Schleyer, *J. Comput. Chem.*, 1983, **4**, 294.
37 J. D. Swalen and J. A. Ibers, *J. Chem. Phys.*, 1962, **36**, 1914.
38 J. A. Pople, M. Head-Gordon and K. Raghavachari, *J. Chem. Phys.*, 1987, **87**, 5968.
39 N. C. Handy and H. F. Schaefer, III, *J. Chem. Phys.*, 1984, **81**, 5031.
40 J. F. Stanton and R. J. Bartlett, *J. Chem. Phys.*, 1993, **98**, 7029.
41 J. F. Stanton, J. Gauss, J. D. Watts, M. Nooijen, N. Oliphant, S. A. Perera, P. G. Szalay, W. J. Lauderdale, S. R. Gwaltney, S. Beck,

A. Balková, D. E. Bernholdt, K.-K. Baeck, P. Rozyczko, H. Sekino, C. Hober, R. J. Bartlett, *ACES II*; Quantum Theory Project: University of Florida, 1997. It includes the integral packages VMOL (J. Almlöf and P. R. Taylor), VPROPS (P. R. Taylor), ABACUS (T. Helgaker, H. J. A. Jensen, P. Jørgensen, J. Olsen and P. R. Taylor).
42 A. J. Sadlej, *Collect. Czech. Chem. Commun.*, 1988, **53**, 1995.
43 A. J. Sadlej, *Theor. Chim. Acta.*, 1991, **79**, 1991.
44 R. A. Marcus, *Annu. Rev. Phys. Chem.*, 1965, **15**, 155; L. Eberson, in *Electron Transfer Reactions in Organic Chemistry*, Springer-Verlag, Berlin, 1987.

Paper 8/05851B